QUANTITATIVE COMPARISONS OF TYPE III RADIO BURST INTENSITY AND FAST ELECTRON FLUX AT 1 AU

R. J. FITZENREITER

Radio Astronomy Branch, Goddard Space Flight Center
Greenbelt, Md., U.S.A.

L. G. EVANS

Computer Sciences Corporation, System Sciences Division
Silver Spring, Md., U.S.A.

and

R. P. LIN

Space Sciences Laboratory, University of California
Berkeley, Calif. U.S.A.

Abstract. We compare the flux of fast solar electrons and the intensity of the type III radio emission generated by these particles at 1 AU. We find that there are two regimes in the generation of type III radiation: one where the radio intensity is linearly proportional to the electron flux, and the second regime, which occurs above a threshold electron flux, where the radio intensity is proportional to the ~2.4 power of the electron flux. This threshold appears to reflect a transition to a different emission mechanism.

1. Introduction

Type III solar radio bursts are generated by fast electrons passing through the plasma of the solar corona and interplanetary medium (Lin *et al.*, 1973). These particles are presumed to excite electron plasma waves which are then converted to electromagnetic radiation through scattering off ion density fluctuations and other plasma waves (Wild, 1950; Ginzburg and Zheleznyakov, 1958). As the fast electrons go outward from the Sun into regions of lower plasma density, the emission shows a characteristic rapid drift to lower frequencies. In the past several years simultaneous spacecraft observations of the fast electrons, the ambient plasma, and the radio and plasma waves generated in the near-Earth interplanetary medium have become available. Since the solar wind plasma at 1 AU is completely ionized and collisionless with $\beta \geqslant 1$ (β = ratio of plasma thermal energy to magnetic energy), these observations are particularly suitable for quantitative studies of the plasma instabilities excited in the passage of fast electrons through a collisionless plasma, and of the wave-wave coupling which produces the electromagnetic radiation.

Previously we identified 10-10^2 keV electrons as the exciters of type III bursts at 1 AU (Lin *et al.*, 1973). The fast electrons were shown to form a peak on the total plasma electron velocity distribution during the burst. This peak results from velocity dispersion (i.e., the arrival of the higher energy electrons at 1 AU before the arrival of lower energy electrons) and drifts to lower energies during the burst

Solar Physics **46** (1976) 437–446.

excitation. In this paper we obtain a quantitative description of the emission processes by comparing the flux of fast electrons with the intensity of the radio emission generated by these particles at 1 AU during individual events.

2. Experimental Details

The particle measurements are from the University of California experiments aboard the IMP-6 spacecraft and Apollo 16 subsatellite which were capable of identifying and measuring the energy spectrum of electrons from 18 to 500 keV, and from 0.5 to 300 keV, respectively. The Goddard Space Flight Center radio experiment on IMP-6 made measurements on 39 discrete frequencies between 30 kHz and 9 MHz. The arrival direction of bursts and information on the source size are obtained by using the modulation imposed on the observed radio flux by the spin of the satellite (Fainberg *et al.*, 1972). Further details of these experiments are contained elsewhere (Lin *et al.*, 1973).

3. Method of Analysis

The electron data were reviewed over a nine month period in 1971 and 1972 to determine the events which had clean onsets. Events that were free from contamination by terrestrial particle fluxes and were intense enough to provide good statistical accuracy were chosen for this study. Approximately twenty particle events were found which satisfied the criteria. A review of the radio data for each of these events was conducted and a type III burst extending to low frequencies was found in every case. However, not all of the radio bursts were suitable for analysis. Interference from other sources, overlapping bursts and saturation of the receivers at low frequencies were the reasons for eliminating some events from further analysis. This left ten bursts for which suitable particle and radio data were available. Figure 1 shows the radio and particle data for one of the events. Figures 1a and 1b are the time profiles of the radio burst intensity and electron flux, respectively, and Figure 1c is the trajectory of the fast electrons determined from the spin modulation on the radio burst profiles at each frequency.

For each event the frequency of the radio emission generated at or near the spacecraft was determined by examining spin modulation in the radio signal. If the spacecraft is surrounded by or very close to the emission region the burst will appear iostropic and thus exhibit no spin modulation. As done previously (Lin *et al.*, 1973), we have identified the first frequency at which the spin modulation disappears as the local emission frequency.

The drift in time of the burst from high to low frequency (Figure 1a) corresponds to the motion of the exciter electrons out from the Sun (Figure 1c); when the electrons reach 1 AU, the local frequency is excited. Thus, an independent determination of local frequency can be obtained from a comparison of the onset

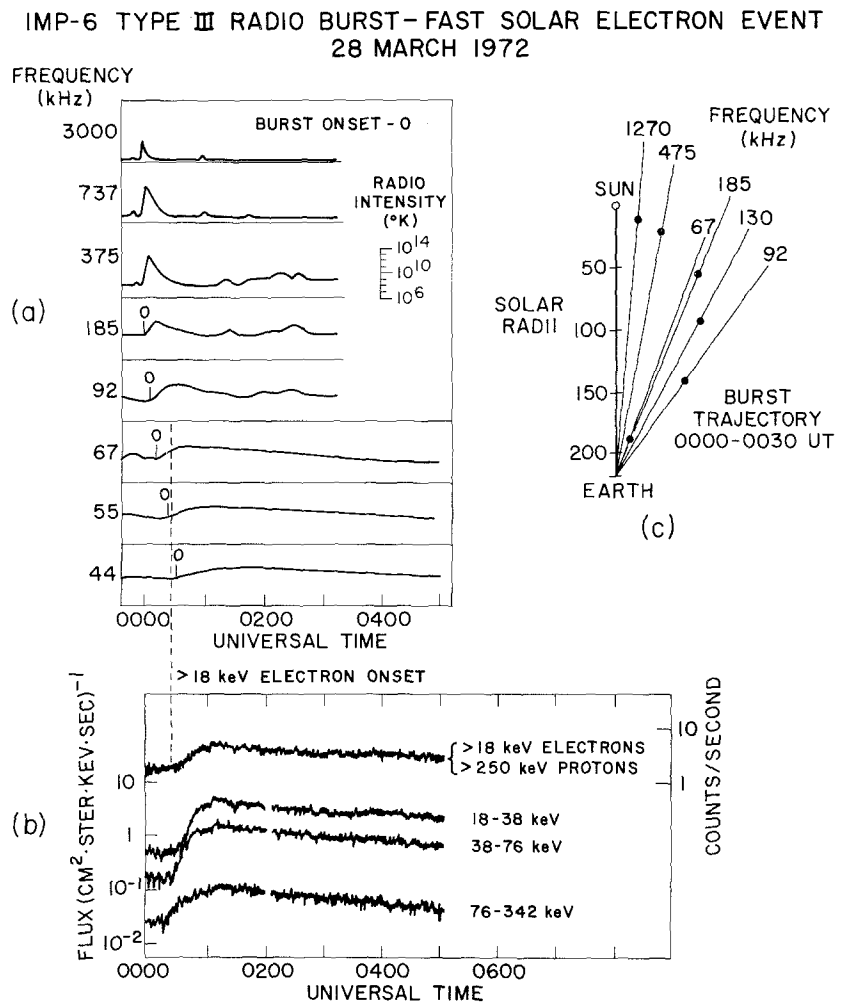

Fig. 1. The type III radio burst (a) observed in coincidence with a fast solar electron event (b) on 28 March 1972. The burst trajectory (c) is obtained from spin modulation of the radio signal. As the fast electrons move out from the Sun along a spiral trajectory, the radio emission drifts to lower frequencies. When the electrons arrive at 1 AU, radio emission originating in the vicinity of the spacecraft is excited. The observing frequency closest to the local emission frequency is 55 kHz as determined by the disappearance of spin modulation and by comparing the burst onset (0) with the onset of the >18 keV electron flux (dashed line).

times. For the burst shown in Figure 1, the onset time at the local frequency, 55 kHz, determined by the disappearance of the spin modulation, coincides with the onset of the electron flux to within the uncertainty in the onset determination. In each of the ten events, the onset of the radio burst at the local emission frequency was closest in time to the observed particle onset. Of the ten events analyzed, nine had local frequencies of either 44 or 55 kHz and one had a local frequency of 30 kHz. This implies a local density (assuming second harmonic emission) of 3–9 cm^{-3} with 6–9 cm^{-3} being the most common for the times of

these events. This is in good agreement with typical solar wind density values at 1 AU (Montgomery *et al.*, 1972).

In order to study the burst emission mechanism we compare the radio intensity to the fast electron flux only during the rising portion of the radio emission, when the decay mechanisms can presumably be neglected. As pointed out previously (Lin *et al.*, 1973), the decay of the radio emission appears to be independent of the electron flux. For each of the events studied, the radio emission reached a maximum before the peak of the >18 keV electron flux. The >18 keV electron flux represents essentially the total fast electron flux effective in producing radio emission since the number of electrons below 18 keV arriving prior to the radio maximum is negligible in all the events.

Figure 2 shows the intensity of the radio emission plotted versus the >18 keV electron flux at 2-min intervals during the rising portion of the radio burst. Since both radio flux and electron flux increase with elapsed time from onset, time in Figure 2 increases with distance of the points from the origin. The background radio emission level was subtracted from all the radio data. A linear relation of these points (on a log-log scale) is obvious. A straight line was fitted to the data by a least-squares technique. Error bars for the particle and radio observations have been included.

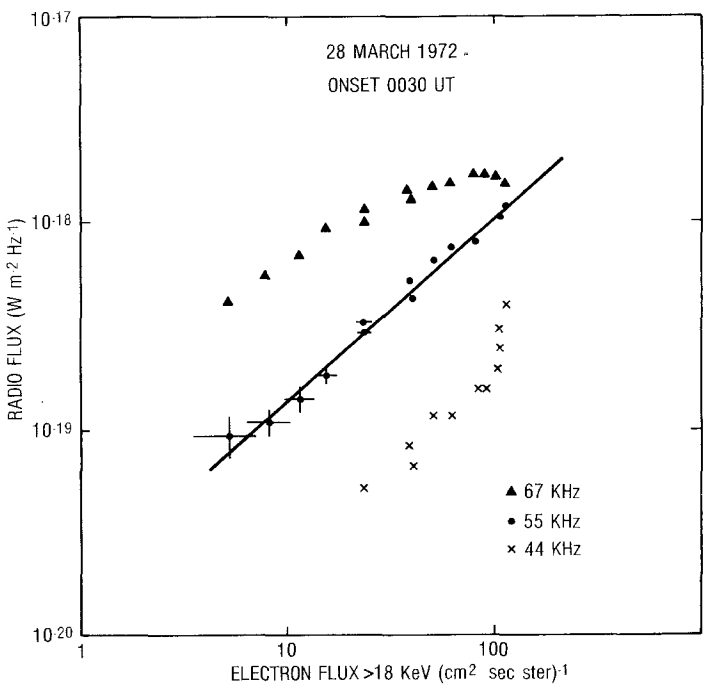

Fig. 2. The dependence of radio intensity on >18 keV electron flux during the rise portion of the burst shown in Figure 1. A least-squares fit to the data (straight line) shows that at 55 kHz, which is the observing frequency closest to the local emission frequency, the radio flux depends on electron flux according to a power law with exponent $\alpha = 0.87$. The power law dependence does not hold, however, for the next highest and next lowest frequencies, 67 kHz and 44 kHz, respectively.

As an additional test of the local frequency determination, plots of radio flux versus electron flux for the next highest and lowest frequencies (67 and 44 kHz, respectively) are also plotted in Figure 2 for this burst. The plots at 67 and 44 kHz show that a linear fit does not hold for frequencies other than the local frequency. It appears that a linear relation (in log-log space) between radio flux and electron flux can thus be used as a check on the determination of the local radio frequency obtained by the radio signal spin modulation and by comparison of onset times. In all of the bursts analyzed, there was complete agreement on the determination of local emission frequency from the various methods.

Similar plots are shown for the remaining nine type III bursts in Figure 3. For most events, a least squares straight line in log-log space gave an excellent fit to the data (Figure 3a–g). Two events, however, could not be fitted well with a straight line. In these cases, the data seemed to be ordered into two linear portions, so a least-squares linear fit was applied to each portion. Different groupings of the points were used, until the best fit was obtained. These double straight line fits are shown in Figure 3(h) and (i).

4. Results

The relationship found in the previous section indicate a power law dependence of the flux of radio emission on patticle flux. The nature of this dependence is important for the theoretical interpretation of the electron-plasma wave interaction in the generation of type III bursts.

The slope of the least-squares fit in Figure 2 gives a value for $\alpha = 0.87$, where $J_R = AJ_E^{\alpha}$. J_R and J_E are the measured radio and electron fluxes, rspectively, and A is a constant. Measurements of the first four bursts shown in Figure 3(a, b, c, d) give similar slopes ($\alpha = 1.13, 1.37, 0.80$, and 1.08 for a, b, c, and d, respectively). Thus, for the five bursts, we obtain an average value of $\alpha = 1.05 \pm 0.20$, which we will assume to be ~ 1 for future discussions.

The next three bursts in Figure 3(e, f, g) have slopes much larger than the first group. However, the slopes are again grouped very closely in value: $\alpha = 2.63$, 2.21, and 2.27 for e, f, and g, respectively, with an average value of $\alpha = 2.37$. These three bursts show a decidedly nonlinear relationship between the radio energy flux and electron flux. Thus, there seems to be a fundamental difference in the emission mechanism for these bursts as compared to the first five bursts described. Some understanding of the nature of this difference can be obtained from an examination of the last two bursts in Figure 3(h, i). These are bursts for which the exponent of the power law changes abruptly at some time after burst onset. The transition occurs during the time between successive data points, within two minutes. The measured values of the slopes for the early part of each burst (the lower straight lines) are equal to 0.84 and 0.92, respectively. The slopes for the later portion of the bursts are 2.38 and 2.54, respectively. Thus the early portions of these bursts are similar to the first group of bursts (Figure 2 and Figure 3, a–d), and the later parts are similar to the second group (Figure 3, e–g).

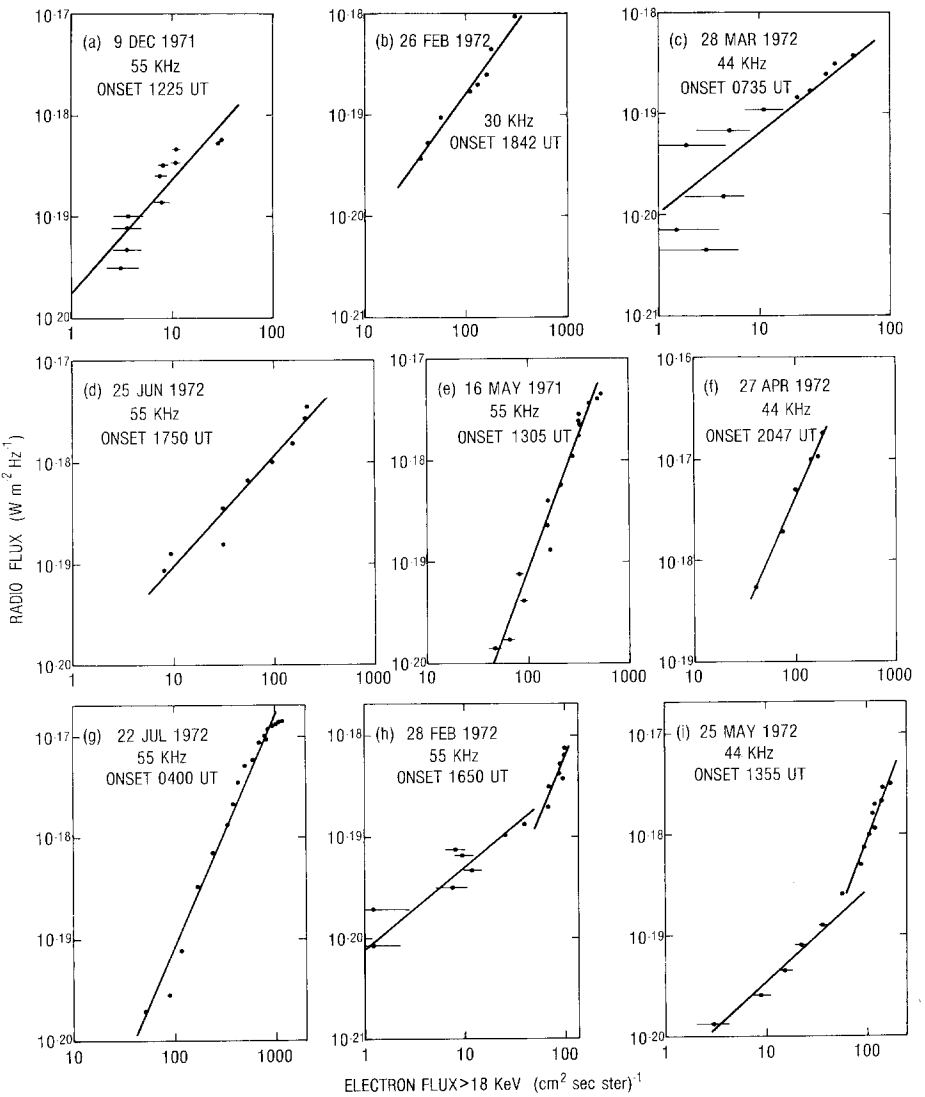

Fig. 3. Nine of the ten events showing a power law dependence of radio flux on electron flux in each case. The tenth event is given in Figure 2. The slopes of the fitted straight lines (equal to the power law index α) fall into two distinct groups. The event in Figure 2 and events a–d have $\alpha \sim 1$; events e–g have $\alpha \sim 2.4$; events h, i show an abrupt transition from $\alpha \sim 1$ to $\alpha \sim 2.4$.

The dependence of radio intensity on electron flux for these ten events is summarized in Figure 4 which shows the range of observed electron flux (from burst onset to burst maximum) plotted against α, the power law exponent. The bursts appear to fall into two groups, one with average $\alpha = 1.0$ and the other with average $\alpha = 2.4$. The dashed lines are the flux levels at which the transition from $\alpha = 1$ to $\alpha = 2.4$ occurs for the bursts shown in Figure 3(h, i). The transition flux for each of these two events and the starting fluxes of the remaining events in the

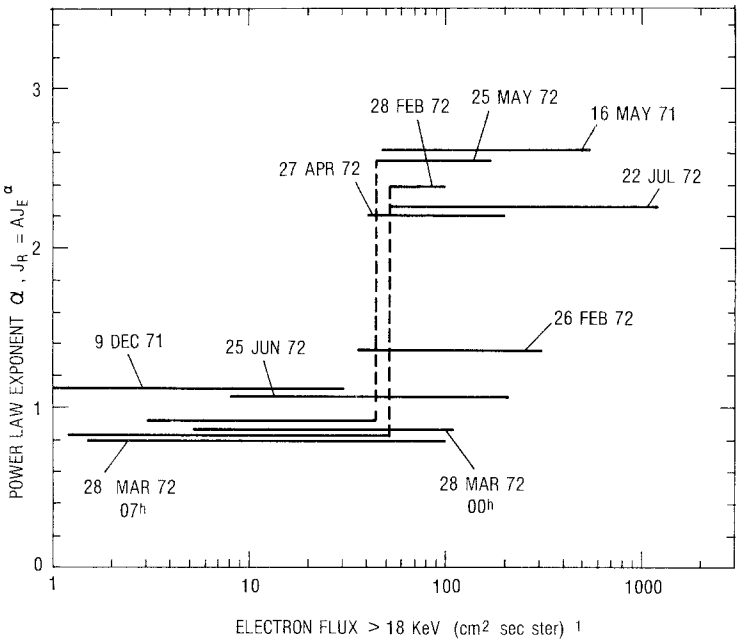

Fig. 4. Range of electron flux (>18 keV) as a function of power law exponent, α, for the ten events. The dashed lines indicate the transitions of the bursts shown in Figures 3h and 3i.

$\alpha = 2.4$ group are nearly the same, approximately 40–50 $(\text{cm}^2\ \text{s sterad})^{-1}$. For most of the events in the $\alpha = 1$ group, the starting flux and most of the flux range in the excitation part of the burst lie well below the transition flux of the $\alpha = 2.4$ group. There is only one event for which the situation is not clear cut, i.e., 26 February, 1972.

The bursts for which a transition is observed suggests that the $\alpha = 1$ and $\alpha = 2.4$ dependences of the bursts which do not show a transition may also be linked together. That is, there may be a transition level for all the events which separates the two regimes of radio emission generation with different functional dependences on electron flux. The transition may not have been observed in all cases because those bursts with $\alpha = 1$ dependence may not have reached the transition, while those with $\alpha = 2.4$ dependence may have already been through transition. Based on the data in Figure 4, the average transition flux for all events is ~ 100 $(\text{cm}^2\ \text{s sterad})^{-1}$.

5. Discussion

Although the functional dependence of the radio emission on electron flux is similar in each group of events, there is a great deal of variability in the intensity of radio emission observed for a given electron flux. For the ten events, the variability in radio intensity is approximately a factor 25 in the $\alpha = 1$ regime, and

approximately a factor 40 in the $\alpha = 2.4$ regime. This can occur for the following reasons:

(1) The observed radio emission originates from a large volume of interplanetary space, while the electron flux is sampled at a single point. Spatial inhomogeneities in the fast electron density in the radio emission region lead to different measured electron fluxes, depending on the point of observation. The observed variability of the transition flux level may also be due to this effect.

(2) A variation in radio source size as well as source distance can lead to different radio intensity measurements.

(3) The radio emission is observed only in a number of narrow band frequency channels. The radio emission generated in situ at the spacecraft may be at a frequency between two of these frequency channels. The possible variation in radio intensity for a given electron flux introduced by this effect can be estimated from Figure 2 and is approximately a factor of 5.

(4) The efficiency for the generation of radio emission should depend on the characteristics of the fast electron population. According to plasma theory the efficiency for generating plasma waves is proportional to the slope, $\partial f/\partial v$, of the rising portion of the peak in the distribution function, $f(v)$, produced by the fast electrons. For a fixed number of fast electrons, this slope will depend on both the spectrum of fast electrons injected at the Sun and the propagation characteristics of the electrons in the interplanetary medium. Softer injection energy spectra and more rapid, less diffusive propagation each have the effect of increasing $\partial f/\partial v$. These effects appear in the observations in two ways. First, the events with softer energy spectra tend to have lower transition flux levels, and second, the radio intensity for a given flux in the nonlinear regime is higher for events with the softer energy spectra and less diffusive propagation.

For these events, the average dependence of radio intensity on electron flux in the linear regime is $J_r = 0.92 \times 10^{-20}\ J_e$ with extreme values of the multiplicative constant being 0.10×10^{-20} and 2.5×10^{-20}. The average dependence in the nonlinear regime is $J_r = 1.8 \times 10^{-23}\ J_e^{2.4}$ with extremes of 0.14×10^{-23} and 6.3×10^{-23} for the constant.

The existence of two distinct regimes of radio emission can be interpreted as a fundamental change in the emission mechanism of type III bursts when the electron flux reaches a critical level. The nature of this change in emission mechanism is not readily explained by most theories. The non-linear dependence of J_r and J_e suggests that radio emission is generated more efficiently after the transition than before. A transition from an incoherent emission mechanism to a more efficient, coherent mechanism can be ruled out as a possible explanation. Lin *et al.* (1973) previously showed that the excitation phase of radio bursts (the rising portion of the intensity time profile) lasts only as long as the peak in the velocity distribution function exists, indicating coherent emission. Calculations also show that typical electron fluxes that are observed in the linear regime are insufficient to produce the observed radio emission by an incoherent process.

One current theory for type III bursts does in fact predict a sudden transition in the radio emission (Papadopoulos *et al.*, 1974; Smith *et al.*, 1975). The transition occurs abruptly at the time of onset of the oscillating two-stream instability. According to this theory, at this time the backward emission of plasma waves becomes intense enough to coalesce with the forward emitted plasma waves, with transformation to electromagnetic radiation occurring more efficiently than before. Preliminary calculations of the transition flux level, using the observed electron distributions and their temporal evolution, are in good agreement with the transition flux levels reported here (R. Smith, private communication).

6. Summary

The flux of fast solar electrons and the intensity of the type III radio emission generated by these particles at 1 AU have been compared. We find that there are two regimes in the generation of type III radiation: one where the radio intensity is linearly proportional to the electron flux, and a second regime, which occurs above a well-defined threshold electron flux, where the radio emission is proportional to the ~2.4 power. This threshold may reflect a transition to a different emission mechanism.

These results are important for the theoretical interpretation of the burst emission process. It is not within the scope of this paper to make a detailed comparison between theory and the observed dependence of radio emission on electron flux in the two regimes. This work is currently underway. In order to better understand the dependence of the observed radio emission on characteristics of the fast electrons, the possible effects of inhomogeneities in the fast electron density and variations in the radio source are also being studied further.

Acknowledgement

We wish to acknowledge very helpful discussions with Drs J. Fainberg, R. A. Smith and M. L. Goldstein. The analysis at the University of California was supported in part by NASA Contract NAS 5-11038.

References

Fainberg, J., Evans, L. G., and Stone, R. G.: 1972, *Science* **178,** 743.
Ginzburg, V. L. and Zheleznyakov, V. V.: 1958, *Soviet Astron. AJ* **2,** 653.
Lin, R. P., Evans, L. G., and Fainberg, J.: 1973, *Astrophys. Lett.* **14,** 191.
Montgomery, M. D., Bame, S. J., and Hundhausen, A. J.: 1972, *J. Geophys. Res.* **77,** 5432.
Papadopoulos, K., Goldstein, M. L., and Smith, R. A.: 1974, *Astrophys. J.* **190,** 175.
Smith, R. A., Goldstein, M. L., and Papadopoulos, K.: 1976, these Proceedings, p. 515.
Wild, J. P.: 1950, *Australian J. Sci. Res.* A**3,** 541.

Discussion

D. Smith: Any idea of the ratio n_{stream} to $n_{\text{background}}$?

Lin: 10^{-7} to 10^{-6}.

Kellogg: How do you get such large numbers for the ratio n_{stream} to $n_{\text{background}}$?

Lin: Take the May 16 event. The flux is approximately 10^3 (cm^2 sterad keV)$^{-1}$. The angular distribution shows only a 2 : 1 anisotropy, so we use 4π steradians and obtain $n_{\text{stream}} = 4\pi \times 10^3/10^{10} \simeq 10^{-6}$ cm^{-3}, compared to solar wind density, $n_{\text{background}} = 5$ cm^{-3}.

Kellogg: What about the range of anisotropy from diffuse to scatter free events?

Lin: There is not too much variation in anisotropies for diffusive versus scatter-free events.

Kellogg: What detectors were used for anisotropy measurements?

Lin: The detector used is only sensitive to >45 keV electrons. It measures an anisotropy of 2 : 1 maximum to minimum.

Kellogg: I agree with your $n_{\text{stream}}/n_{\text{background}}$ when I use 4π sterad.

D. Smith: Does the anisotropy change as the event progresses?

Lin: Not too much, although there is poor time resolution in the anisotropy measurements.

Kellogg: In the May 16 event, the magnetic field was connected to the bow shock?

Lin: Yes, although there are no clear indications that connection to the bow shock has any effect on these results.

Kellogg: These fluxes are measured by the telescope detector?

Lin: Yes.